

Research Article

Microstructure and Mechanical Properties of Vacuum Hot Pressed P/M Short Steel Fiber Reinforced Aluminum Matrix Composites

S. Jain, K. Chandra, and V. Agarwala

Metallurgical and Materials Engineering Department, Indian Institute of Technology, Roorkee 247667, India

Correspondence should be addressed to S. Jain; sidharthjai@gmail.com

Received 2 December 2013; Accepted 9 January 2014; Published 4 May 2014

Academic Editors: K. Hokamoto, P. Karjalainen, and Y. Sun

Copyright © 2014 S. Jain et al. This is an open access article distributed under the Creative Commons Attribution License, which permits unrestricted use, distribution, and reproduction in any medium, provided the original work is properly cited.

Commercial purity aluminum powder of irregular shape and ligamental morphology having average particle size of $75\ \mu\text{m}$ was blended with medium carbon steel short fibers having average diameter of $100\ \mu\text{m}$ and maximum length up to $1000\ \mu\text{m}$. The green compacts of pure aluminum and reinforced compositions were hot-pressed in 10^{-3} torr vacuum, at 723 K, 773 K, and 823 K for 5, 10, and 15 min durations under 50 MPa axial stress on Gleeble 3800 simulator. Microstructures of the sintered composites have been studied by scanning electron microscopy (SEM) and energy dispersive X-ray analysis (EDAX). The sintered compacts were characterized for densification behavior, hardness, and growth of Fe_xAl_y reaction interface. Positive densification parameter was achieved for up to 10 wt.% reinforcement fraction. The maximum hardness of 51 Hv was achieved for 10 wt.% at 823 K for 15 min sintering time. The reaction interface was analysed by scanning electron microscopy (SEM) and energy dispersive X-ray analysis (EDAX). The reaction interface was found to be composed of Fe_3Al , FeAl_2 , Fe_2Al , Fe_3Al , Fe_4Al , Fe_2Al_5 , and FeAl intermetallics. Growth of the reaction interface was diffusion-controlled which followed a nearly parabolic law with a rate constant of $1.41 \times 10^{-12}\ \text{m}^2\ \text{s}^{-1}$ at 823 K.

1. Introduction

Powder metallurgical (P/M) processing is based on blending of matrix powders and reinforcing elements (particles, platelets, or whiskers), secondary working operations like forging, extrusion and hot pressing [1, 2]. P/M methods offer the ability to modify the chemistry and retain control over the matrix-reinforcement interface. The sintering of aluminum is difficult due to the presence of thermodynamically stable oxide shell on the particle surface which hinders wetting and diffusion [3]. Several approaches have been suggested to overcome this problem: addition of 0.1–1.0 wt.% Mg [1, 3, 4], addition of Sn and Zn to facilitate transient liquid phase filling of porosities [1, 3–5], sintering above the melting point of aluminum [6], and sintering in nitrogen atmosphere [7]. Diffusion, plastic flow, and power-law creep have been identified as the dominant mechanisms for densification by hot isostatic pressing (HIP) sintering [8]. Vacuum hot pressing

(VHP) is found to enhance the sintering rate and final density of the compact in solid-state sintering, by providing additional stress at elevated temperature, whilst avoiding sintering aids and special atmospheres. P/M processed Al/SiC composites, with up to 30 vol.% SiC, were realized by VHP to full density [8]. Several workers have pursued the continuous reinforcement of aluminum alloys by stainless steel or steel wires using liquid metallurgical processes, to offer a cost-competitive improvement in overall properties of monolithic aluminum alloys. Investigations have shown the formation and uncontrolled growth of a complex intermetallic reaction interface (RI) of type Fe_xAl_y , composed of Fe_3Al , FeAl , FeAl_2 , Fe_2Al_5 , and FeAl_3 phases [9–15].

In this investigation, commercially pure aluminum powder ($\sim 75\ \mu\text{m}$) has been blended with short steel fibers, cold compacted into green preforms for further hot consolidation using vacuum hot pressing. The developed composites have been analyzed for densification, hardness, and

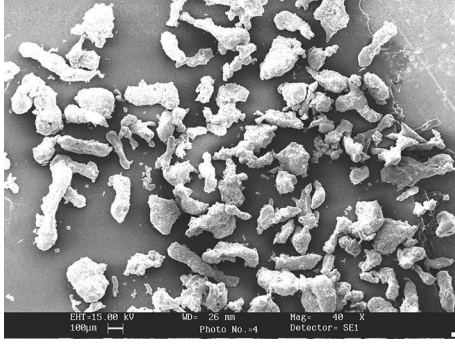


FIGURE 1: SEM image of aluminum powder.

microstructural examination on scanning electron microscope (SEM). The thickness of the reaction interface has been analyzed by EDAX.

2. Experimental Procedure

2.1. Materials and Processing. Commercially pure aluminum powder of nominal chemical composition (wt.%) given in Table 1 is used as the matrix material. The average particle size was $75\ \mu\text{m}$ with irregular shape and ligamental morphology as shown in Figure 1, having a nominal density of $2.63\ \text{g cm}^{-3}$. Short steel fiber, reinforcement used in phenolic brake pads, with an average diameter $100\ \mu\text{m}$ and $500\text{--}1000\ \mu\text{m}$ length, having a chemical composition as given in Table 2, with a nominal density of $7.83\ \text{g cm}^{-3}$ (Figure 2(a)) and a semicircular cross section as shown in Figure 2(b), was the reinforcement. The sieve analysis of fibers is given in Table 3. The short steel fiber was cleaned with acetone, dried in an oven, and hand-mixed with aluminum powder. The mixture of aluminum with short steel fiber, designated as Al5SSF, Al10SSF, and Al15SSF, for respective weight fractions of reinforcement was blended in a horizontal tumble jar mill using ceramic balls of $16\ \text{mm}$ diameter, with a ball to composite weight ratio of 1:1, to avoid agglomeration of fibers, while ensuring that the fiber aspect ratio was maintained; a uniform distribution was obtained after 2 h of milling at 80 rpm. As received, aluminum powder (designated as Al.) was also subject to the same milling cycle.

The composite blends were uniaxially cold-compacted using a hardened steel die in a hydraulic press of $25\ \text{kN}$ capacity at $375\ \text{MPa}$ to prepare cylindrical green preforms of $16\ \text{mm}$ diameter and $24\ \text{mm}$ length. Stearic acid dissolved in acetone was used as the die wall lubricant. The green compacts of pure aluminum and all reinforced compositions were hot pressed in 10^{-3} torr vacuum, at $723\ \text{K}$, $773\ \text{K}$, and $823\ \text{K}$ for 5, 10, and 15 min durations, under $50\ \text{MPa}$ maximum axial stress on Gleeble 3800 thermomechanical simulator using a set of cylindrical die and punches made of H 13 hot die steel, as shown in Figure 3. Gleeble 3800 system utilizes the resistance of the specimen for heating by controlling the flow of current through the specimen, to an accuracy of $\pm 1\ \text{K}$ across the specimen cross section. Cr-Al thermocouple was welded to the outer wall of the die for temperature measurements.

TABLE 1: Composition of pure aluminum powder (wt.%).

Si	Fe	Ti	V	Cu	Mn	Al
0.08	0.15	0.001	0.007	0.001	0.003	Bal.

TABLE 2: Composition of short steel fibers (wt.%).

C	Mn	Si	S	P	Fe
0.38	0.52	0.10	0.02	0.024	Bal.

TABLE 3: Sieve analysis of short steel fibers.

ASTM sieve number	Size (μm)	% retained (30 min)
+16		Nil
-16 +25	1190	2
-25 +60	707	3
-60 +100	250	15
-100 +300	149	35
-300	50	45

Heating rate was maintained at $5\ \text{K s}^{-1}$. A representative hot pressing cycle is shown in Figure 4. Hot pressing stress was applied as a linearly increasing function with sintering time, with maximum stress at the end of sintering cycle. The sintered compacts were allowed to cool in vacuum. The die allowed a 0.25% diametric expansion during hot pressing. Graphite paste was used as the parting agent. A LVDT was used to measure the axial dimension changes to an accuracy of $\pm 0.001\ \text{mm}$; all parameters were logged at a $100\ \text{s}^{-1}$ data acquisition rate.

2.2. Characterization. Green density of the cold-compacted preforms was determined by dimensional measurements to an accuracy of $0.01\ \text{mm}$ and weight measurements to an accuracy of $0.1\ \text{mg}$. Density measurements were carried out after vacuum hot pressing by water immersion technique. Vickers hardness was determined using diamond indenter at $5\ \text{Kg}$ load for $10\ \text{s}$ on FIE Instruments (India) hardness tester. The average of 5 measurements was reported. FEI QUANTA model 200F FESEM with EDAX was used for microstructure and reaction interface analysis.

3. Results and Discussions

3.1. Densification. Green densification behaviour for Al-5SSF is shown in Figure 5. The relative density, ratio of green density to theoretical density, decreased with the increase in reinforcement as shown in Figure 6 for all compositions cold-compacted at $375\ \text{MPa}$. Uniaxial cold compaction can be described as a two-stage process wherein compaction is followed by relaxation on account of elastic recovery. The high elastic modulus of short steel fibers relative to aluminum matrix aids in relaxation due to higher elastic recovery. The fibers also act as barriers to self-shearing of hard alumina layer on irregular aluminum particles during

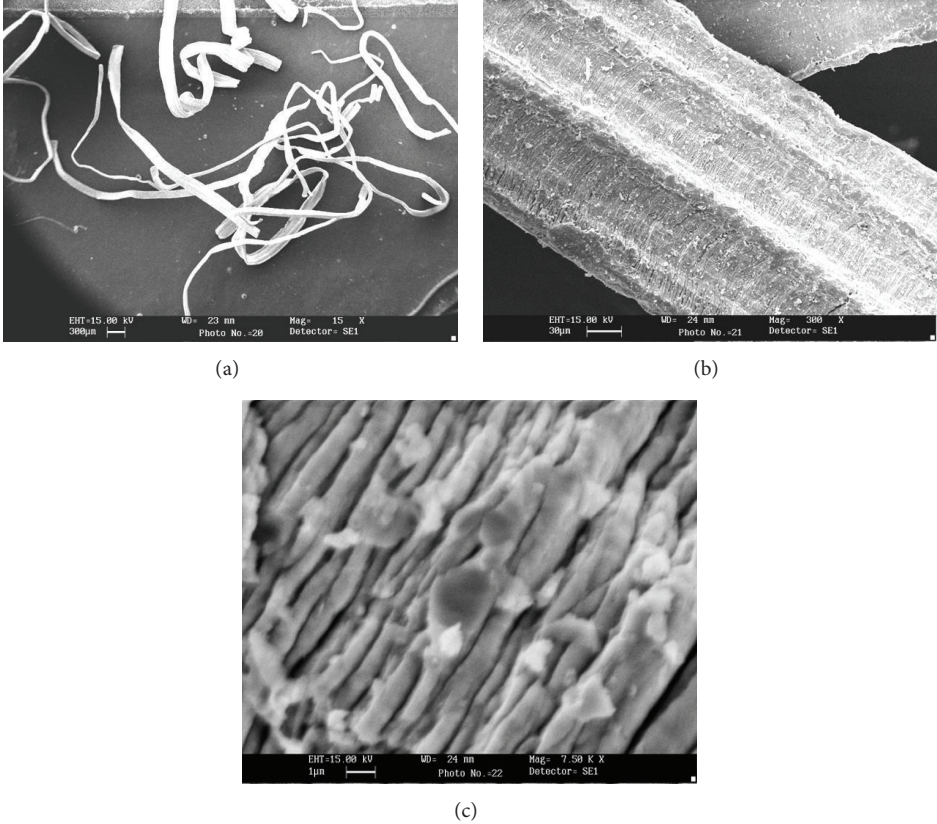


FIGURE 2: SEM micrographs of (a) short steel fibers, (b) fiber cross section, and (c) fiber surface.

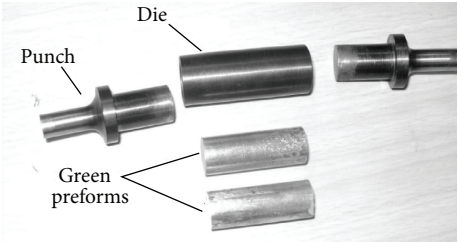


FIGURE 3: Die and punches used for VHP on Gleeble 3800 thermomechanical simulator.

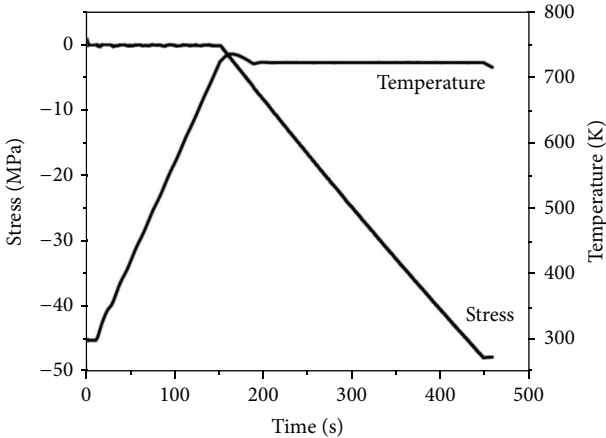


FIGURE 4: Time synchronous plot of sintering temperature and hot pressing stress.

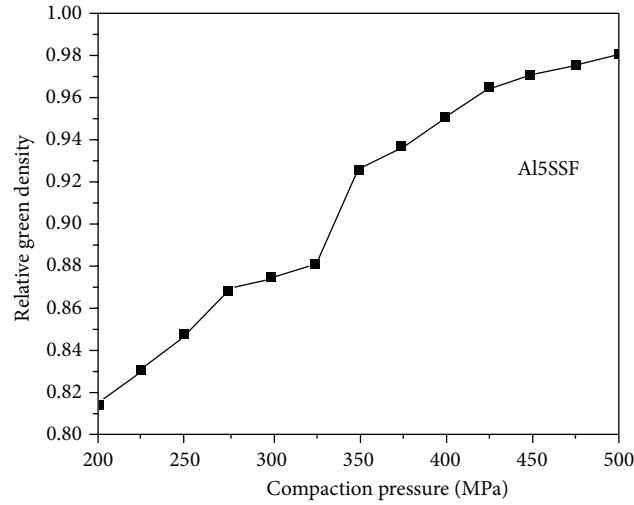


FIGURE 5: Cold compaction behaviour of Al5SSF.

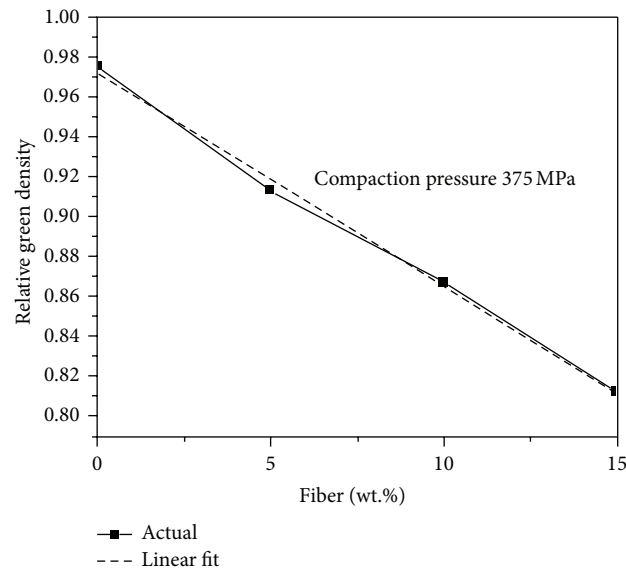


FIGURE 6: Relative green density dependence on fiber wt.%.

cold compaction. Relative density of green compacts follows a linear relation with reinforcement weight fraction, given by

$$\left(\frac{\rho_g}{\rho_t}\right) = 0.97114 - 0.0106(R), \quad (1)$$

where ρ_g is the green density, ρ_t is the theoretical density, ρ_s is the sintered density, and R is the reinforcement weight fraction. As shown in Figure 7, relative sintered densities for compacts vacuum hot pressed and sintered at 723 K for 5 min under 50 MPa also follow a linear relation with reinforcement weight fraction, given by

$$\left(\frac{\rho_s}{\rho_t}\right) = 0.99162 - 0.00832(R). \quad (2)$$

The change in density as a result of vacuum hot pressing and sintering is characterized by the densification parameter, defined as

$$\phi = \frac{(\rho_s - \rho_g)}{(\rho_t - \rho_g)}. \quad (3)$$

Densification parameter with (wt.%) reinforcement and theoretical and sintered densities for vacuum hot pressed and sintered preforms at 5 min and 50 MPa is shown in Figure 8. Positive values indicate porosity reduction and net densification resulting from sintering. It can be seen that positive values are obtained up to 10 wt.% fiber fraction. Figure 9 shows a net expansion of the green compact during heating for first 150 s of the cycle without hot pressing, indicative of a net expansion. After the sintering temperature

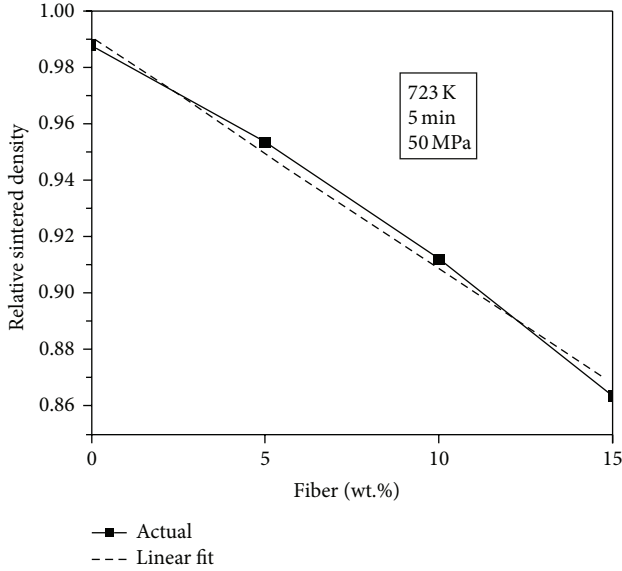


FIGURE 7: Relative sintered density.

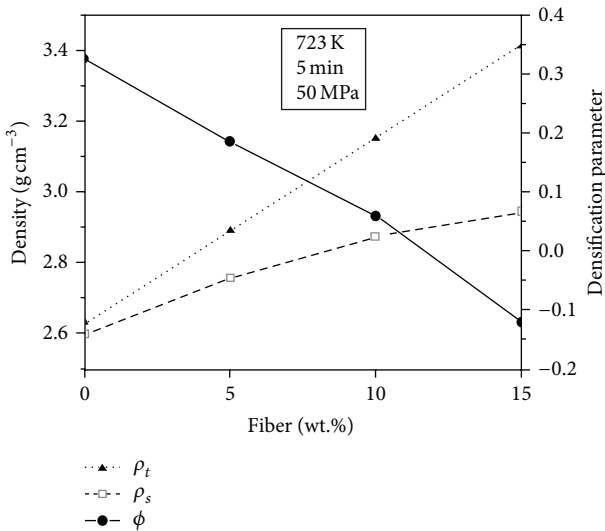


FIGURE 8: Densification parameter dependence on Fiber wt.%.

is attained and a linearly increasing stress is applied, a net contraction is achieved resulting in densification. Diffusion, plastic flow, and power-law creep have been reported as the dominant mechanisms for densification by hot pressing during sintering [8].

3.2. Hardness. Bulk hardness is an important parameter for optimizing the weight fraction of the reinforcement and determination of optimum processing parameters like sintering time and temperature. Figures 10(a)–10(d) show the dependence of sintering time and temperature on Vickers hardness of unreinforced and all reinforced compositions. There is an increase in hardness as a result of reinforcement for all sintering temperatures and times. The maximum

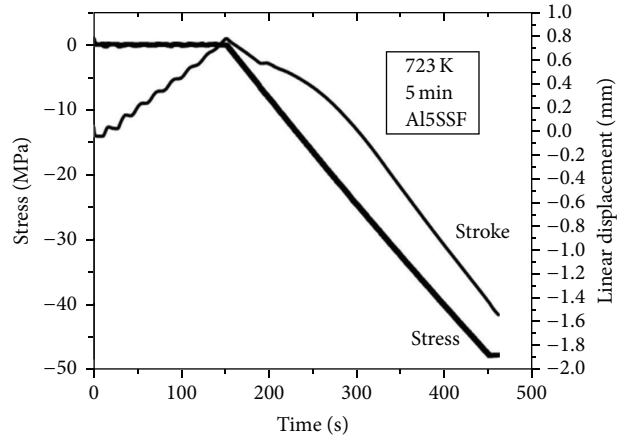


FIGURE 9: Linear displacement of the specimen under hot pressing stress.

hardness of 51 Hv is achieved for Al10SSF at 823 K for 15 min duration.

3.3. Characterization of Reaction Interface and Determination of Growth Kinetics. A steady growth of the reaction interface was observed in Al10SSF composite vacuum hot pressed at 823 K under 50 MPa linearly increasing stress. The sintered compacts were sectioned in a plane perpendicular to the axis of the cylindrical specimen for characterization of the reaction interface by scanning electron microscope equipped with energy dispersive X-ray analysis (EDAX). Line scans along the steel fibers confirmed the presence of a reaction interface formed as a result of interdiffusion of Fe and Al. Figures 11(a)–11(d) show the line scans for Fe and Al. From the intensity counts, it is possible to establish the presence of Fe₃Al (Figure 11(a)), FeAl₂, Fe₂Al (Figure 11(b)), Fe₃Al, Fe₄Al (Figure 11(c)), Fe₂Al₅, FeAl (Figure 11(d)), and other nonstoichiometric intermetallics. To analyze the interface growth mechanism, the thickness *d* of the interface was plotted against the square root of hot pressing time *t*^{1/2}, as shown in Figure 12. The straight line in the central portion of the curve indicates that the growth of the interface follows a parabolic law (*d*² = *kt*), which is indicative of a diffusion controlled mechanism; *k* is the temperature depended parabolic rate constant [14]. The value of *k* can be determined from the slope of the straight line portion of the curve as shown in Figure 12, *k* = 1.41 × 10⁻¹² m² s⁻¹ at 823 K. This value is about 10 times higher than that obtained by Hwang et al. for vacuum hot pressing of aluminum foil-stainless steel wire composite at 873 K, 70 Mpa, and about 4 times higher than that obtained by Bhagat for stainless steel wire-P/M aluminum composite vacuum hot pressed at 800 K, 140 MPa. This higher value of the rate constant can be attributed to resistive heating of the compact, wherein the flowing current encountered steel fibers of higher specific resistivity than the aluminum matrix, leading to localized hot spots dispersed evenly within the compact. Comparative studies have been conducted in radiant heating environments. Thickness of the reaction interface is an important consideration for metal-metal MMC

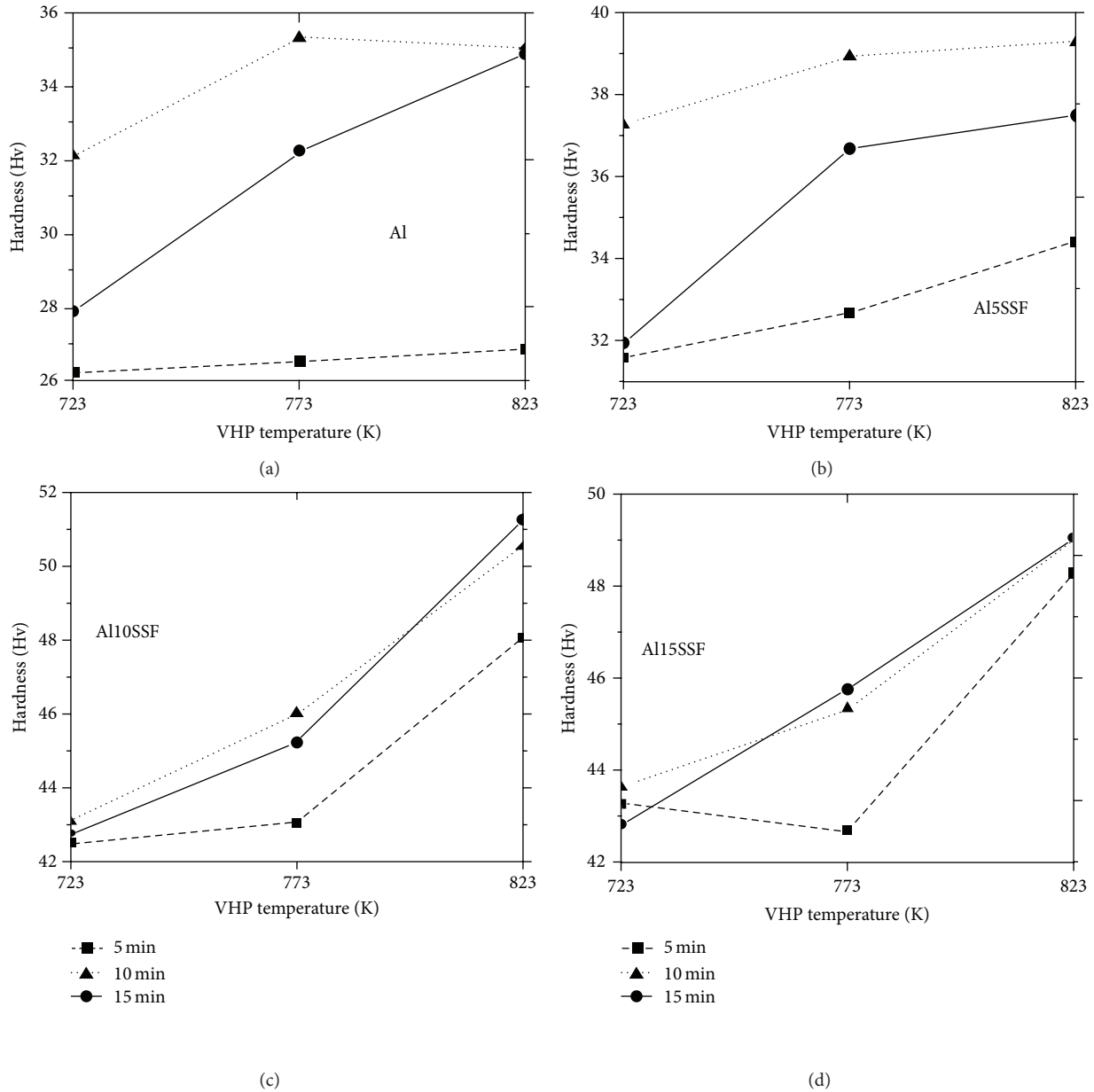
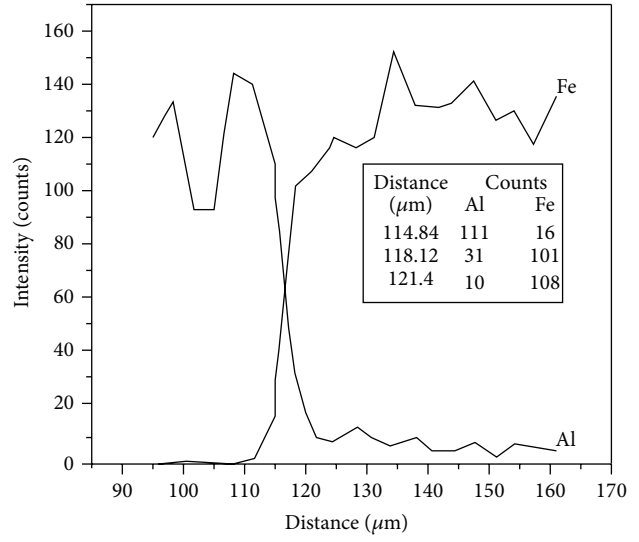
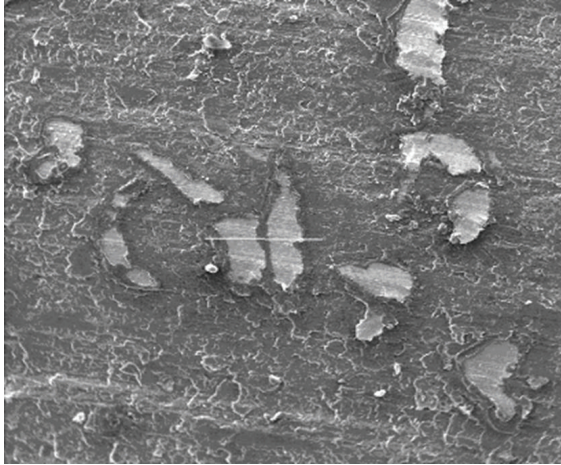


FIGURE 10: (a–d) Dependence of hardness (Hv) on vacuum hot pressing and sintering time and temperature.

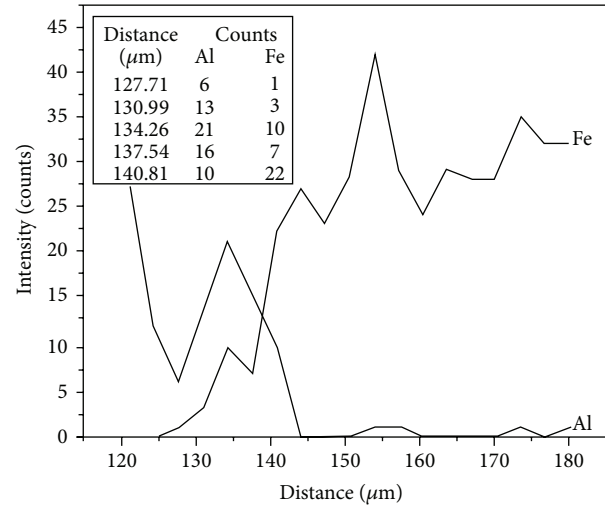
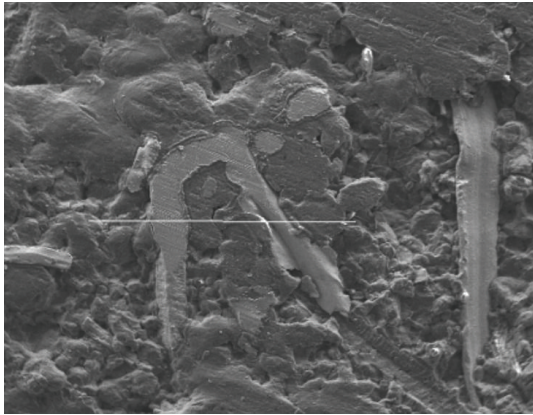
systems; a well interfaced composite can give much superior properties by synergistic effects arising from effective load transfer from the weak matrix to the strong reinforcement; however, the intermetallic nature of the RI leads to excessive hardness, low ductility, susceptibility to crack propagation, and environmental embrittlement. Patented literature for manufacture of steel wire mesh reinforced cast aluminum connecting rods [16] has reported an optimum RI of $2\text{--}10\ \mu\text{m}$, achieved by carbonitriding treatment of wire mesh prior to melt infiltration. Vortex cast short steel fiber reinforced aluminum based composites investigated by Mandal et al. suggested Cu coating of the fibers for improved wetting and inhibition of RI growth. However, in the present work near optimum RI has been obtained without pretreatment of the fibers.

4. Conclusions

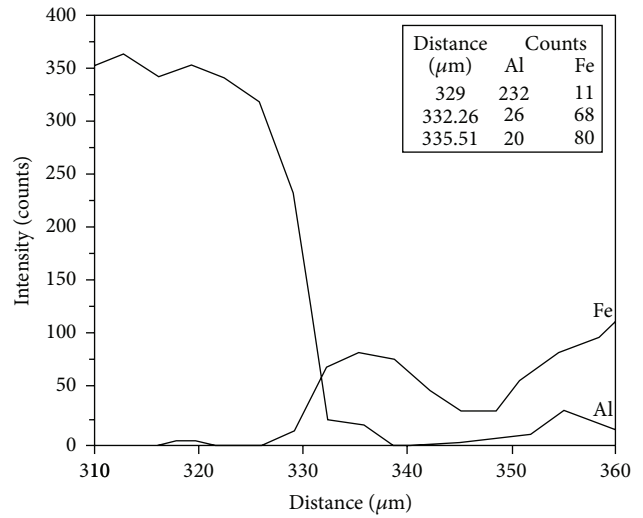
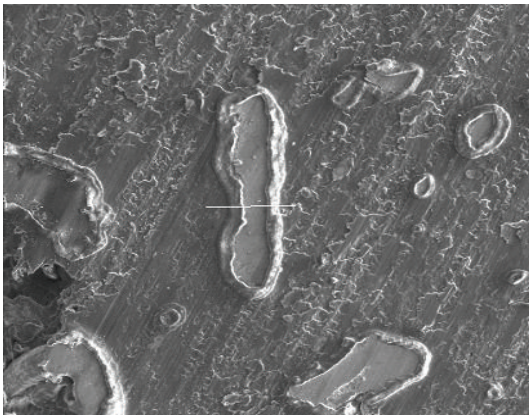
Aluminum matrix short steel fiber reinforced composites were developed using preforming vacuum hot pressing and sintering technique. Resistive heating was found to be more effective than traditional methods of heating as evident by the high rate constant of reaction at the fiber matrix interface. Limitations associated with sintering of aluminum were overcome by vacuum hot pressing and sintering below the melting point. Powder metallurgical processing allows control of the reaction interface and an optimum thickness of intermetallic phase was obtained without any alteration of reinforcement surface or chemistry. Critical reinforcement weight fraction was determined to be 10%. Linearly increasing stress at sintering temperature enabled densification plastic flow, diffusion,



(a)

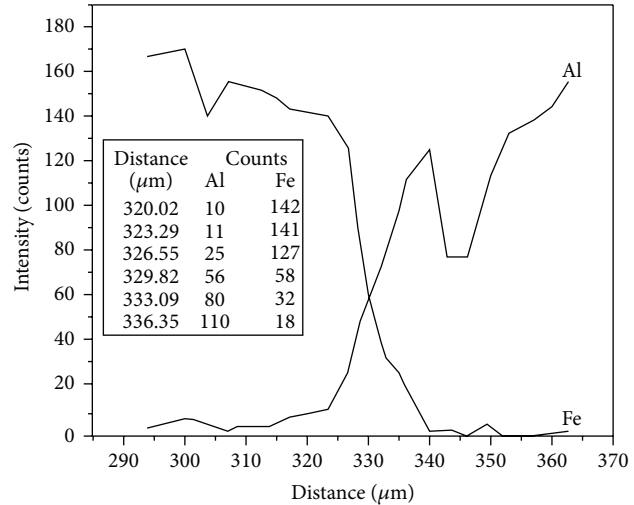
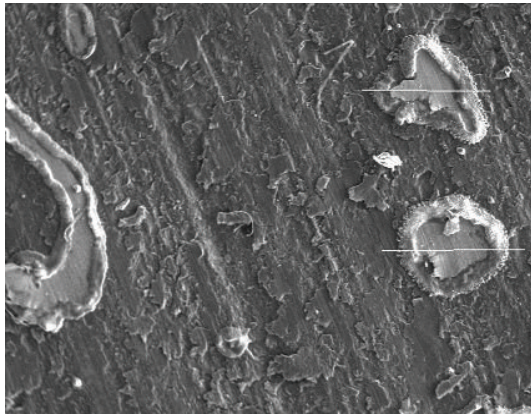


(b)



(c)

FIGURE II: Continued.



(d)

FIGURE 11: SEM micrographs with corresponding EDAX line scans of vacuum hot pressed and sintered Al₁₀SSF compacts showing effect of sintering time: (a) 5 min, (b) 10 min, (c) 15 min, and (d) 20 min on growth of Al_xFe_y reaction interface.

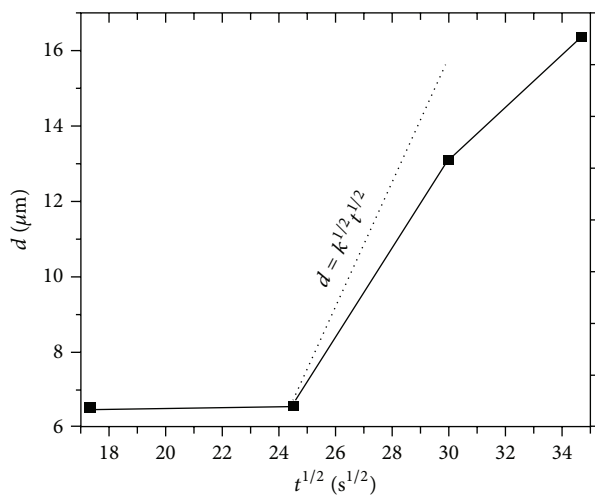


FIGURE 12: Variation of interface thickness d (μm) with $(\text{time})^{1/2}$ at 823 K.

and power law creep. The metal-metal MMC system developed in this work needs to be further characterized for strength, elevated temperature behavior, and tribological characteristics for a cost competitive alternative to dominant ceramic reinforcement.

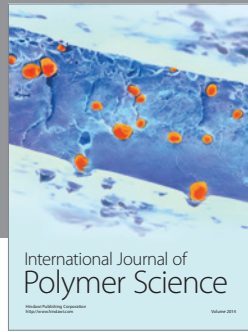
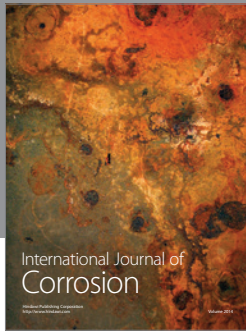
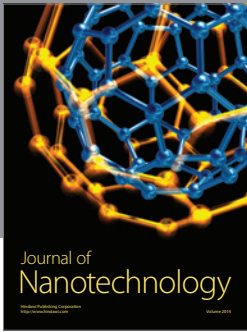
Conflict of Interests

The authors declare that there is no conflict of interests regarding the publication of this paper.

References

- [1] D. Huda, M. A. El Baradie, and M. S. J. Hashmi, "Metal-matrix composites: manufacturing aspects. Part I," *Journal of Materials Processing Technology*, vol. 37, no. 1-4, pp. 513-528, 1993.
- [2] J. W. Kaczmar, K. Pietrzak, and W. Włosiński, "Production and application of metal matrix composite materials," *Journal of Materials Processing Technology*, vol. 106, no. 1-3, pp. 58-67, 2000.
- [3] M. Rosso, "Ceramic and metal matrix composites: routes and properties," *Journal of Materials Processing Technology*, vol. 175, no. 1-3, pp. 364-375, 2006.
- [4] Z. Y. Liu, T. B. Sercombe, and G. B. Schaffer, "The effect of particle shape on the sintering of aluminum," *Metallurgical and Materials Transactions A: Physical Metallurgy and Materials Science*, vol. 38, no. 6, pp. 1351-1357, 2007.
- [5] T. B. Sercombe, "On the sintering of uncompacted, pre-alloyed Al powder alloys," *Materials Science and Engineering A*, vol. 341, no. 1-2, pp. 163-168, 2003.
- [6] G. B. Schaffer, J.-Y. Yao, S. J. Bonner, E. Crossin, S. J. Pas, and A. J. Hill, "The effect of tin and nitrogen on liquid phase sintering of Al-Cu-Mg-Si alloys," *Acta Materialia*, vol. 56, no. 11, pp. 2615-2624, 2008.
- [7] T. B. Sercombe, "On the sintering of uncompacted, pre-alloyed Al powder alloys," *Materials Science and Engineering A*, vol. 341, no. 1-2, pp. 163-168, 2003.
- [8] T.-W. Kim, "Determination of densification behavior of Al-SiC metal matrix composites during consolidation processes," *Materials Science and Engineering A*, vol. 483-484, no. 1-2, pp. 648-651, 2008.
- [9] S. K. Mannan, V. Seetharaman, and V. S. Raghunathan, "A study of interdiffusion between AISI type 316 stainless steel and aluminium," *Materials Science and Engineering*, vol. 60, no. 1, pp. 79-86, 1983.
- [10] S. N. Tiwari, A. N. Tiwari, and V. Gopinathan, "High temperature interfacial studies in aluminium-stainless steel composites," *Journal of Materials Science*, vol. 22, no. 8, pp. 2680-2684, 1987.
- [11] R. B. Bhagat, "High pressure squeeze casting of stainless steel wire reinforced aluminium matrix composites," *Composites*, vol. 19, no. 5, pp. 393-399, 1988.

- [12] R. B. Bhagat, "Growth kinetics of interface intermetallic compounds in stainless steel fibre reinforced aluminium matrix composites," *Journal of Materials Science*, vol. 24, no. 4, pp. 1496–1502, 1989.
- [13] Y.-H. Hwang, C.-F. Horng, S.-J. Lin, K.-S. Liu, and M.-T. Jahn, "Interface study for stainless steel fibre-reinforced aluminium matrix composite," *Journal of Materials Science*, vol. 32, no. 3, pp. 719–725, 1997.
- [14] R. C. Agarwala, V. Agarwala, and L. M. Garg, "Garg production of reinforced castings containing stainless steel wires in Aluminium alloy," *Berg Und Huttenmannische Monatshefte*, vol. 143, no. 3, supplement, pp. S.86–S.89, 1998.
- [15] V. Agarwala, K. G. Satyanarayana, and R. C. Agarwala, "Studies on the development of aluminium alloy-mild steel reinforced composite," *Materials Science and Engineering A*, vol. 270, no. 2, pp. 210–218, 1999.
- [16] B. E. Yoon and M. H. Kim, "Reinforced material for an automobile connecting rod," United States Patent 5523171, 1996.



Hindawi

Submit your manuscripts at
<http://www.hindawi.com>

